International Journal of Automotive and Mechanical Engineering (IJAME)
ISSN: 2229-8649 (Print); ISSN: 2180-1606 (Online); Volume 11, pp. 2272-2281, January-June 2015

DOI: http://dx.doi.org/10.15282/ijame.11.2015.10.0191

TEMPERATURE ANALYSIS WHEN USING ETHYLENE-GLYCOL-BASED TIO_2 AS A NEW COOLANT FOR MILLING

M. Yogeswaran[1*], K. Kadirgama[1,2], M.M. Rahman[1,2] and R. Devarajan[1,2]

[1]Faculty of Mechanical Engineering, Universiti Malaysia Pahang,
26600 Pekan, Pahang, Malaysia
[*]Email: mustafizur@ump.edu.my
Phone: +6094246239; Fax: +609424622
[2]Automotive Engineering Centre, Universiti Malaysia Pahang,
26600 Pekan, Pahang, Malaysia

ABSTRACT

This paper presents the effects of various milling conditions on the tool wear and workpiece temperature when using ethylene-glycol-based TiO_2 nanofluid as the coolant for stainless steel AISI 304. A TiN coated carbide insert is used as the milling tool. A thermocouple was embedded into the workpiece to record the workpiece temperature during the end-milling process. It can be clearly seen that the temperature keeps on increasing after each experimental pass for three sets of experiments. The experiment conducted using the ethylene-glycol-based TiO_2 nanocoolant exhibits a much lower workpiece temperature compared to the experiment conducted using a normal commercial coolant. Milling with the ethylene-glycol-based TiO_2 nanocoolant reduced the wear on the edge of the insert compared to the normal commercial coolant. In conclusion, end-milling stainless steel AISI 304 using a TiN coated carbide insert and an ethylene-glycol-based TiO_2 nanocoolant exhibits superior results with regard to workpiece temperature and tool wear. The temperature was reduced by 30 percent when using the nanofluid

Keywords: Milling; TiO_2 nanocoolant; tool wear; ethylene-glycol; workpiece temperature.

INTRODUCTION

The metal machining process is important in metal shaping to produce parts. Milling is one of the most commonly used machining processes in industry for metal removal. Milling is mostly used in the automotive, aerospace and manufacturing industries. As well as the manufacturing cost, in the metal removal process, tool wear and workpiece temperature are important factors in measuring the quality of a product. The relation between high temperature and poor machinability directly contribute to high tool wear and poor surface finish [1-4]. The thermal effects are particularly relevant when milling stainless steel due to it being tougher, and gummier and having a tendency to work harden very rapidly[5]. When a workpiece is milled, a huge amount of the work of the milling machine is converted into heat [6]. The heat generated increases the temperature of the cutting tool and the workpiece and contributes to machining defects such as tool wear, thermal expansion and also to the poor dimension tolerance. Matsumoto, Barash [7] stated that at a high cutting speed, 80% of the heat generated during machining is carried away by the chip. However, the maximum temperature is formed at the rake face

which is placed some distance away from the tool nose before the chip is flushed away [8]. A cutting fluid is a liquid which is used to produce cooling and lubrication between the cutting tool and the work piece. The cutting fluid also reduces the contact processes in the chip formation zone. Cooling and lubrication are very important in the cutting process. Accordingly, the lubricant action is very important at a low cutting speed and the cooling is important at higher cutting speeds due the high increases in heat in the cutting zone [9]. Water has been used as a cooling medium in various machining operations [10-13]. However, although water is an excellent cooling medium due to its high thermal conductivity, it corrodes the part and is a poor lubricant. Nowadays, oils and synthetic fluids are used as coolants in machining. Four types of cutting fluid are used today: straight or neat oils, soluble oil, synthetic fluids and semi-synthetic fluids. Around 80% of the cutting fluids in industry incorporate water based oil and synthetic fluids as the coolant in machining [14].

Nanofluid is a fluid which is suspended with nanoparticles. The nanoparticles will suspend in conventional fluids such as water, ethylene glycol (EG) and engine oil. Nanofluids are thought to be the next generation heat transfer fluids due to their existing properties [15-18]. Nanofluids have attracted great interest in various industries, such as the micro electric, automotive, and manufacturing. According to Khaleduzzaman, Sohel [19] the advantages of nanofluids over micro-sized fluids are their better stability and the particle size. Additionally, nanofluids achieve higher thermal conductivity than the base liquid. More than 20 laboratories worldwide have published data on the thermal conductivity of nanofluids. All the results show that the thermal conductivity of nanofluids exhibits higher thermal properties, even the concentration of liquid is less than 5% in volume percentage [17, 18, 20, 21]. The viscosity of nanofluids is another important property in heat transfer applications. As reported by Mehrali, Sadeghinezhad [22], the pH value and viscosity of nanofluids are considered as factors that affect their stability at room temperature. Therefore, a study has been conducted to evaluate the effect of various milling conditions, cutting speeds, feed rates and depth of cut, on the tool wear and workpiece temperature by using EG-based TiO_2 nanofluid as the coolant. The tool wear and workpiece temperature have been compared with milling results using a normal commercial coolant.

EXPERIMENTAL SET UP

Design of Experiment

Stainless steel AISI 304 blocks were used throughout the experiment. The size of each block was 180×100×25 mm. The hardness of these blocks is around Rockwell B 70. The chemical composition of the workpiece material is shown in Table 1 (Krishna et al., 2006) and the properties of the workpiece material are shown in Table 2. The milling inserts are made by Ceratizit from ISO XDKT 11T308SR-F50. They are of a coated carbide grade with a TiN chemical vapor deposition (CVD) coating. TiN is considered to be very ductile because it is relatively hard. The TiN coating is 3 μm thick. The insert used in this study is X-shaped and is slotted into a 32 mm diameter tool holder. It is specified for use in flooded machining. A standard water-soluble coolant was used as the flood coolant in this study. The cutting inserts used in this experiment are shown in Figure 1 where d = 4.9 mm, l_1 = 1.2 mm, l = 7.8 mm, $\alpha = 15^o$, d_1 = 2.5 mm and s = 3.18 mm.

Table 1. Chemical composition of workpiece material.

Element	C	Si	Mn	Cr	Mo	P	S	Ni
Wt %	0.02	0.32	1.31	16.4	2.03	0.30	0.20	12.17

Table 2. Physical properties of workpiece material [23].

Properties	Value
Density (kg/m^3)	8000
Elastic Modulus	193
Mean Coefficient of Thermal Expansion (μm/m/^{o}C)	17.8
Thermal Conductivity at 100^{o}C	16.2
Thermal Conductivity at 500^{o}C	21.5
Specific Heat (J/kg.K)	500

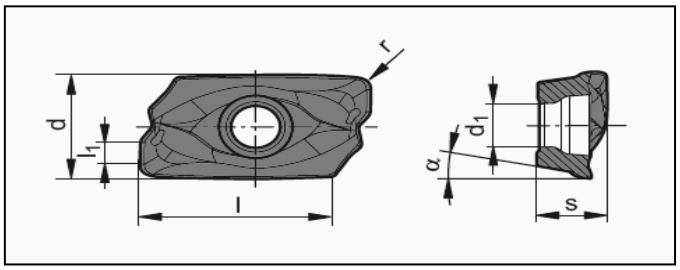

Figure 1. TiN coated carbide insert from ISO XDKT 11T308SR-F50.

All the machining was carried out on an HAAS CNC milling machine. Machining was undertaken using three varying cutting parameters: cutting speed, feed rate and depth of cut. Suitable combinations of the cutting parameters were used to deduce the design of the experiment using the Box–Behken method with three factors. A total of 15 combinations of experiments were undertaken. The length of each cut was 180 mm. Milling was carried out in one direction with three varying axial depths, feed rates and cutting speeds, respectively. All the experiments used the up milling process (the rotation of the spindle against the direction of the feed) [24].The transient workpiece temperature was measured using a K-type thermocouple. The two thermocouple wires are encapsulated as shown in Figure 2. The encapsulated end of the thermocouple wire is embedded into the workpiece as shown in Figure 3. The other end of the thermocouple wire was connected to an eight-channel data logger to record the temperature during the milling process. The intervals of the readings recorded by the data logger are fixed at 1.0 s. Four thermocouples are located along the central line of the milling process on the workpiece to take readings throughout the workpiece material. The thermocouple is located 10 mm below the milling zone to detect the workpiece temperature. The experimental setup is shown in Figure 2 and illustrated schematically in Figure 3.

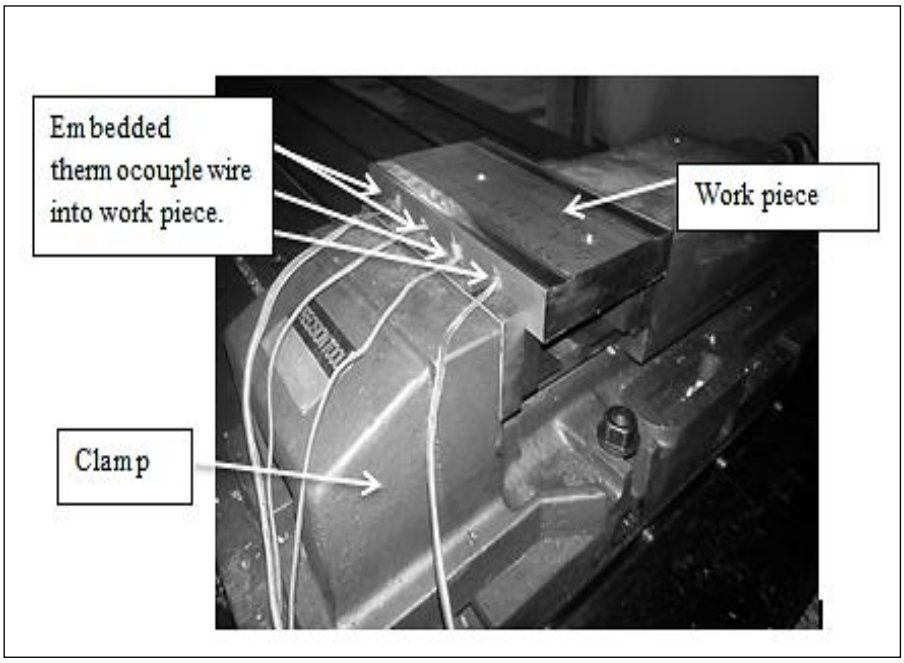

Figure 2. Workpiece temperature measurement and clamping of the workpiece.

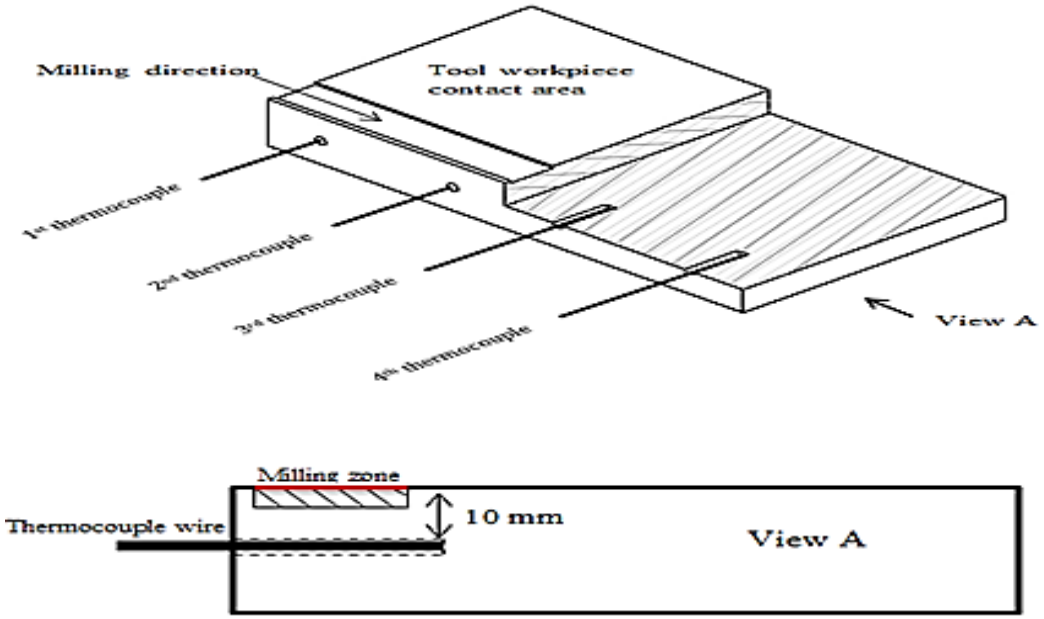

Figure 3. Schematic and section view of workpiece used to measure the temperature.

RESULTS AND DISCUSSION

Figure 4 illustrate the temperature reading for three passes of the milling experiment at high, medium and low cutting speeds. The cutting condition for each experiment is shown in Table 3. It can be clearly seen that the temperature keeps on increasing after each experimental pass for the three sets of experiments. The temperature for the high cutting speed experiment after the first experimental pass is approximately 27.8 ºC and it increase to 29 ºC after three experimental passes. In addition, the temperature for the

medium cutting speed experiment after the first experimental pass is 27.3 ºC increasing to 28.3 ºC. Meanwhile, at the low cutting speed, the temperature after the first experimental pass is approximately 27.2 ºC increasing to 27.6 ºC. It can be seen that the workpiece temperature rises much higher at the high cutting speed compared to the low cutting speed. As stated earlier, this is due to the increase in friction force which contributes to the increase in cutting temperature. Therefore, the workpiece temperature also increases [25]. As can be seen in Figure 5, the temperature begins to increase a few seconds after the milling process begins, and it continues to increase gradually during the milling cycle and reaches the maximum temperature. It can also be observed that, the workpiece temperature does not reach a steady state during the milling process.

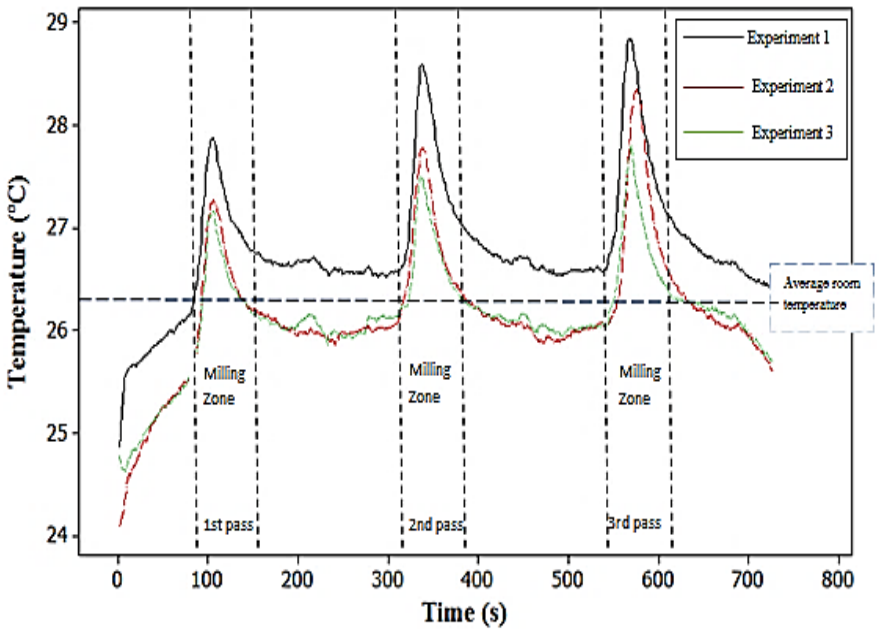

Figure. 4. Workpiece temperature for three passes of the milling experiment at high, medium and low cutting speeds by using a normal commercial coolant.

Throughout the cooling state, the workpiece temperature decreases gradually until it reaches room temperature. The milling cycle condition is similar for the first, second and third passes of the milling experiment. In addition, Figure 5 shows that the workpiece temperature increases gradually with increases in the milling passes. This is due to the excessive temperature on the rake face of the tool perhaps contributing to the wear on the face of the milling tool [26]. Therefore, after each experimental milling pass the tool became blunt. Hence, the heat generated in the milling zone will be much higher after each pass conducted. Finally, the heat penetrating into the workpiece will also be higher [27]. One can see the higher measured workpiece temperature value of the end-milling stainless AISI 304 is 29 ºC, which is relatively low compared to the current research using an infrared camera. These phenomena occur because the heat spreads throughout the workpiece and the high gradient before it is detected by the thermocouple sensor. Therefore, using the thermocouple technique to measure the workpiece temperature during milling indicated the whole body temperature which was useful in estimating the absorbed energy [28].

Table 3. Cutting condition.

Experiment	Level	Cutting Speed (rpm)	Feed Rate (mm/tooth)	Depth of Cut (mm)
1	High	2500	0.04	0.2
2	Medium	2000	0.03	0.2
3	Low	1500	0.03	0.1

Figure 5 shows the workpiece temperature for single-pass milling for high, medium and low cutting speeds using an EG-based TiO_2 nanocoolant. It indicates that the workpiece temperature increase is much higher at the high cutting speed compared to the low. For high-cutting-speed milling, at 2500 rpm, the workpiece temperature rises to 25.3 ˚C. However, the workpiece temperature just rises to 24.7 ˚C for the low cutting speed and 25.0 ˚C for the medium. This clearly indicates that the cutting speed is directly proportional to the workpiece temperature. Conversely, when compared to the experiment conducted between a normal commercial coolant and the EG-based TiO_2 nanocoolant, it clearly shows that the EG-based TiO_2 nanocoolant exhibits a much lower workpiece temperature of approximately 9% lower than the normal commercial coolant [29]. Figure 5 also shows some sudden drops in the temperature when conducting the milling experiment with EG-based TiO_2 nanocoolant. This is due to the high thermal conductivity of the nanoparticles which flow away from the heat from the cutting zone, so avoiding a huge amount of heat penetrating into the workpiece during the milling experiment [30, 31].

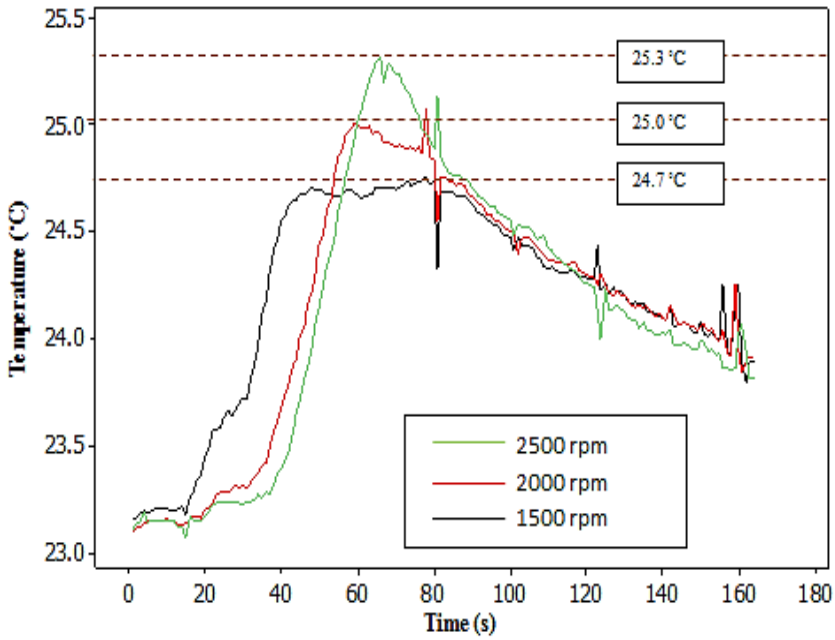

Figure 5. Workpiece temperature for the single-pass milling experiment at high, medium and low cutting speeds using an ethylene-glycol-based TiO_2 nanocoolant.

Figure 6 shows four different milling conditions, low cutting speed and high cutting speed together with two different milling coolants, normal commercial coolant and EG-based TiO_2 nanocoolant, for 540 mm of milling. The figure confirms that there

is a huge different in the wear of the inserts when using an EG-based TiO_2 nanocoolant compared to the normal commercial coolant. The insert used for the milling using a normal commercial coolant starts to exhibit some flank wear on the edge of the inserts. This is due to the huge amount of heat penetrating into the inserts during the milling and contributes the earlier wear. However, the insert used for milling using the EG-based TiO_2 nanocoolant shows less wear and a layer of nanoparticles covered the edge of the inserts. On the other hand, the high cutting speed contributes to earlier damage on the inserts compared to the low cutting speed. This is because the high friction between the workpiece and the milling insert contributes to the high temperature in the milling zone.

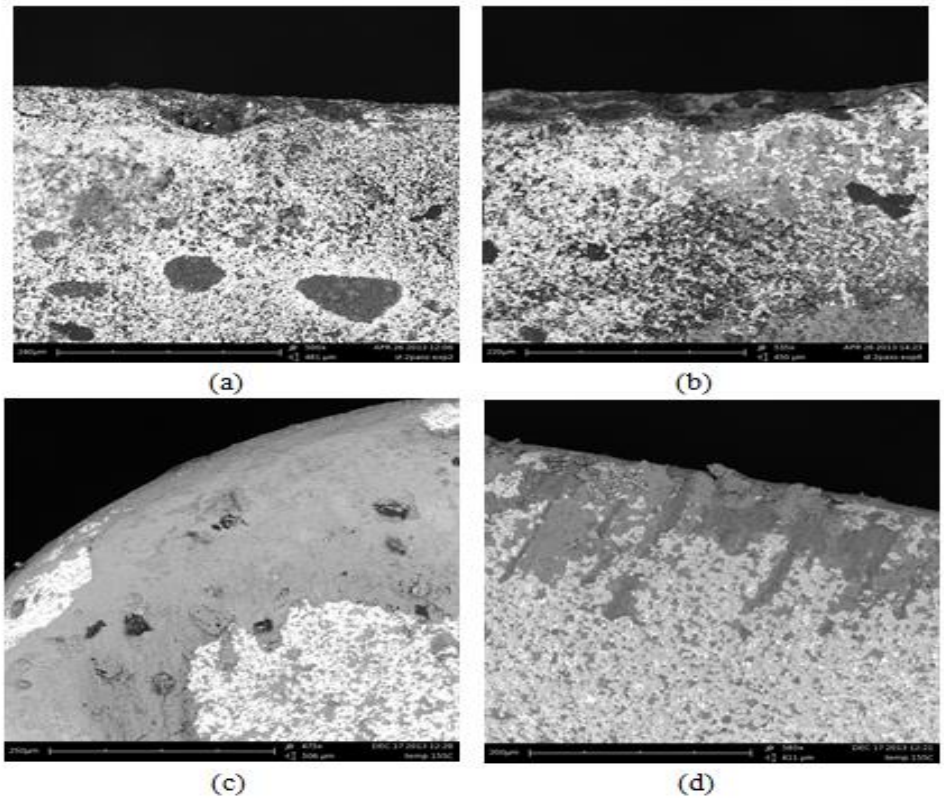

Figure 6. SEM capture of the cutting insert under four different milling conditions: (a) cutting speed: 1500 rpm with commercial coolant; (b) cutting speed: 2500 rpm with commercial coolant; (c) cutting speed: 1500 rpm with ethylene-glycol-based TiO_2 nanocoolant and (d) cutting speed: 2500 rpm with ethylene-glycol-based TiO_2 nanocoolant.

CONCLUSIONS

In conclusion, end-milling of stainless steel AISI 304 using a TiN coated carbide insert with an EG-based TiO_2 nanocoolant exhibits superior results with regard to the workpiece temperature and also tool wear. There is a reduction in workpiece temperature of about 9% compared to milling using a normal commercial coolant. In addition, the tool wear from milling using the EG-based TiO_2 nanocoolant is much less and the tool life is increased. This shows that nanoparticles reduce the damage on the edge of the tool by reducing the heat penetrating into the inserts. However, this experiment is limited, since the workpiece temperature could not be simulated using the

thermocouple method. This can be overcome in the future by using a thermal camera to detect the workpiece temperature. Therefore, the actual tool temperature and workpiece temperature can be observed in parallel in order to study the temperature distribution in end-milling.

ACKNOWLEDGEMENTS

Author would like to thanks Universiti Malaysia Pahang and Malaysian Higher Education Ministry for providing grant under RDU RDU110373 to conduct the research.

REFERENCES

[1] Chen YG, Lu WZ, Xu J, Zhu YS, Zuo DW. Investigation of surface integrity on TC4-DT in high speed grinding with CBN wheel. Advanced Materials Research. 2014; 1027: 140-5.

[2] Singh R. Comparison of statistically controlled machining solutions of titanium alloys using USM. International Journal of Automotive and Mechanical Engineering. 2010;1:66-78.

[3] Najiha MS, Rahman MM, Yusoff AR, Kadirgama K. Investigation of flow behavior in minimum quantity lubrication nozzle for end milling processes. International Journal of Automotive and Mechanical Engineering. 2012;6:768-76.

[4] Najiha MS, Rahman MM, Yusoff AR. Modeling of the End Milling Process for Aluminum Alloy AA6061t6 using HSS Tool. International Journal of Automotive and Mechanical Engineering. 2013;8:1140-50.

[5] Kim JH, Park CH. Effect of milling temperature on nanoclusters and ultra fine grained microstructure of oxide dispersion strengthened steel. Journal of Alloys and Compounds. 2014;585:69-74.

[6] Liu L, Zhang S, Zhang J, Liu JP, Xia W, Du J, et al. Highly anisotropic SmCo 5 nanoflakes by surfactant-assisted ball milling at low temperature. Journal of Magnetism and Magnetic Materials. 2015;374:108-15.

[7] Matsumoto Y, Barash M, Liu C. Effect of hardness on the surface integrity of AISI 4340 steel. Journal of Manufacturing Science and Engineering. 1986;108:169-75.

[8] Pusavec F, Deshpande A, Yang S, M'Saoubi R, Kopac J, Dillon OW, et al. Sustainable machining of high temperature Nickel alloy–Inconel 718: part 2–chip breakability and optimization. Journal of Cleaner Production. 2015;87:941-52.

[9] Murshed S, Leong K, Yang C. Investigations of thermal conductivity and viscosity of nanofluids. International Journal of Thermal Sciences. 2008;47:560-8.

[10] Das SK. Nanofluids—the cooling medium of the future. 2006.

[11] Kadirgama K, Rahman MM, Ismail AR, Bakar RA. Finite element analysis of HASTELLOY C-22HS in end milling. Journal of Mechanical Engineering and Sciences. 2011;1:37-46.

[12] Najiha MS, Rahman MM, Kamal M, Yusoff AR, Kadirgama K. Minimum quantity lubricant flow analysis in end milling processes: A computational fluid

dynamics approach. Journal of Mechanical Engineering and Sciences. 2012;3:340-5.
[13] Che Ghani SAB, Cheng K, Minton T. Back chip temperature in environmentally conscious turning with conventional and internally cooled cutting tools. Journal of Mechanical Engineering and Sciences. 2013;4:356-72.
[14] Yu W, France DM, Choi SU, Routbort JL. Review and assessment of nanofluid technology for transportation and other applications. Argonne National Laboratory (ANL); 2007.
[15] Wang X, Xu X, S. Choi SU. Thermal conductivity of nanoparticle-fluid mixture. Journal of Thermophysics and Heat Transfer. 1999;13:474-80.
[16] Mahendran M, Lee GC, Sharma KV, Shahrani A. Performance of evacuated tube solar collector using water-based titanium oxide nanofluid. Journal of Mechanical Engineering and Sciences. 2012;3:301-10.
[17] Azmi WH, Sharma KV, Mamat R, Anuar S. Nanofluid properties for forced convection heat transfer: An overview. Journal of Mechanical Engineering and Sciences. 2013;4:397-408.
[18] Hussein AM, Sharma KV, Bakar RA, Kadirgama K. Heat transfer enhancement with nanofluids – A review. Journal of Mechanical Engineering and Sciences. 2013;4:452-61.
[19] Khaleduzzaman S, Sohel M, Saidur R, Mahbubul I, Shahrul I, Akash B, et al. Energy and exergy analysis of alumina–water nanofluid for an electronic liquid cooling system. International Communications in Heat and Mass Transfer. 2014;57:118-27.
[20] Tongkratoke A, Pramuanjaroenkij A, Chaengbamrung A, Kakac S. Numerical study of nanofluid heat transfer enhancement with mixing thermal conductivity models. Computational Thermal Sciences: An International Journal. 2014;6.
[21] Liu J, Wang F, Zhang L, Fang X, Zhang Z. Thermodynamic properties and thermal stability of ionic liquid-based nanofluids containing graphene as advanced heat transfer fluids for medium-to-high-temperature applications. Renewable Energy. 2014;63:519-23.
[22] Mehrali M, Sadeghinezhad E, Latibari ST, Kazi SN, Mehrali M, Zubir MNBM, et al. Investigation of thermal conductivity and rheological properties of nanofluids containing graphene nanoplatelets. Nanoscale Research Letters. 2014;9:1-12.
[23] Eitssayeam S, Intatha U, Rujijanagul G, Pengpat K, Tunkasiri T. Structural and electrical properties characterization of (1–x) PbZr0. 52Ti0. 48O3–xBaFe0. 5Nb0. 5O3 system. Applied Physics A. 2006;83:295-9.
[24] Antony J. Design of experiments for engineers and scientists: Elsevier; 2014.
[25] Singh D, Chaturvedi V. Investigation of optimal processing condition for abrasive water jet machining for stainless steel AISI 304 using grey relational analysis coupled with S/N ratio. Applied Mechanics and Materials. 2014; 592-594: 438-43.
[26] Nguyen T, Kwon P, Kang D, Bieler T. The Root Cause of Nose and Flank Wear and Their Behavior in Turning Ti-6Al-4V With Carbides and PCD Inserts. ASME 2014 International Manufacturing Science and Engineering Conference collocated with the JSME 2014 International Conference on Materials and Processing and the 42nd North American Manufacturing Research Conference: American Society of Mechanical Engineers; 2014. p. V002T02A47-VT02A47.

[27] Chinchanikar S, Choudhury S. Machining of hardened steel—Experimental investigations, performance modeling and cooling techniques: A review. International Journal of Machine Tools and Manufacture. 2015;89:95-109.
[28] Kadirgama K, Abou-El-Hossein K, Mohammad B, Habeeb H. Numerical and statistical model to determine temperature and heat distribution when machining Hastelloy C-22HS. International Journal of Statistics & Economics. 2007;1:24-41.
[29] Rahman M, Kadirgama K, Ab Aziz AS. Artificial neural network modeling of grinding of ductile cast iron using water based SiO2 nanocoolant. International Journal of Automotive and Mechanical Engineering. 2014;9:1649-61.
[30] Murshed SS, de Castro CN. Superior thermal features of carbon nanotubes-based nanofluids–A review. Renewable and Sustainable Energy Reviews. 2014;37:155-67.
[31] Shokoohi Y, Khosrojerdi E, Shiadhi BR. Machining and ecological effects of a new developed cutting fluid in combination with different cooling techniques on turning operation. Journal of Cleaner Production. 2015;94:330-9.